

J.E. STALNAKER^{1,✉,*}
S.A. DIDDAMS¹
T.M. FORTIER^{1,2}
K. KIM^{1**}
L. HOLLBERG¹
J.C. BERGQUIST¹
W.M. ITANO¹
M.J. DELANY¹
L. LORINI¹
W.H. OSKAY¹
T.P. HEAVNER¹
S.R. JEFFERTS¹
F. LEVI^{1,***}
T.E. PARKER¹
J. SHIRLEY¹

Optical-to-microwave frequency comparison with fractional uncertainty of 10^{-15}

¹ National Institute of Standards and Technology, Time and Frequency Division, MS 847, Boulder, CO 80305, USA

² Los Alamos National Laboratory, P-23 Physics Division, MS H803, Los Alamos, NM 87545, USA

Received: 19 June 2007
© Springer-Verlag 2007

ABSTRACT We report the technical aspects of the optical-to-microwave comparison for our recent measurements of the optical frequency of the mercury single-ion frequency standard in terms of the SI second as realized by the NIST-F1 cesium fountain clock. Over the course of six years, these measurements have resulted in a determination of the mercury single-ion frequency with a fractional uncertainty of less than 7×10^{-16} , making it the most accurately measured optical frequency to date. In this paper, we focus on the details of the comparison techniques used in the experiment and discuss the uncertainties associated with the optical-to-microwave synthesis based on a femtosecond laser frequency comb. We also present our most recent results in the context of the previous measurements of the mercury single-ion frequency and arrive at a final determination of the mercury single-ion optical frequency: $f(\text{Hg}^+) = 1\,064\,721\,609\,899\,145.30(69) \text{ Hz}$.

PACS 06.30.Ft; 42.62.Eh; 32.30.Jc

1 Introduction

The development of stabilized femtosecond laser frequency combs (FLFCs) has dramatically simplified the absolute measurement of optical frequencies [1, 2]. By providing the necessary division of optical frequencies at hundreds of terahertz to rf and microwave atomic frequency standards at the gigahertz frequency range, frequency combs have made measurements of optical frequencies routine (for reviews,

see [3, 4]). However, only a few absolute frequency measurements [5–12] have been made at levels approaching the uncertainty of the best cesium (Cs) fountain frequency standards. Achieving such accuracies is an essential step in the development of the next generation of optical frequency standards.

This paper discusses the technical details of the comparison process and the optical-to-microwave synthesis used in the most recent measurement (March 2006) of the mercury ion (Hg^+) optical frequency standard relative to the microwave Cs fountain frequency standard, NIST-F1. Here we focus on the techniques used to relate the two frequencies, discuss limitations on the optical-to-microwave conversion process, and compare the uncertainties arising in the measurement process to those of the frequency standards. We also summarize all of the measurements of the Hg^+ frequency standard and arrive at a final fractional uncertainty of 6.9×10^{-16} . This uncertainty is within a factor of 1.5 of the current uncertainty in the NIST-F1 frequency standard [13, 14] and currently represents the most accurate determination of an optical frequency.

2 Experiment

We present the discussion of the optical-to-microwave frequency comparison in the context of our most recent measurement of the Hg^+ frequency relative to the Cs frequency standard. An overview of the frequency comparison method is shown in Fig. 1. The experiment spans three laboratories in the same building. The various components are linked by appropriate cables and noise-canceled optical fibers [15]. The frequency of the Hg^+ standard is measured by use of the optical-to-microwave conversion provided by the FLFC. The light used in the Hg^+ experiment is interfered with that of the FLFC to form a heterodyne beat signal between the Hg^+ light and a single optical mode of the FLFC. This beat signal is used to phase lock the frequency of a single mode of the FLFC. With the carrier-envelope offset frequency also stabilized, the repetition rate of the FLFC is directly related to the

✉ Fax: +1-440-775-6379, E-mail: jason.stalnaker@oberlin.edu

*Current address: Department of Physics and Astronomy, Oberlin College, 110 N Professor St., Oberlin, OH 44074, USA

**Current address: School of Mechanical Engineering, Yonsei University, 134 Shinchon-dong, Seodaemun-gu, Seoul 120-749, Korea

***Current address: Istituto Nazionale di Ricerca Metrologica, Strada delle Cacce 91, 10135 Torino, Italy

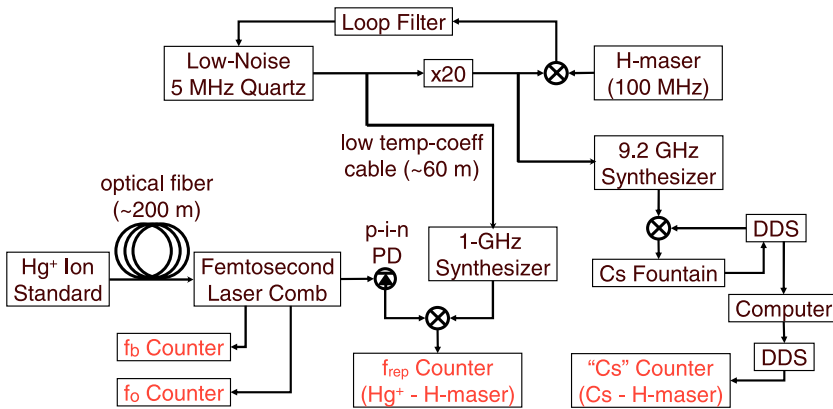


FIGURE 1 Block diagram showing the relations of the frequencies used in the Hg^+ /Cs comparison. The frequency of the DDS is combined with the output of the 9.2 GHz synthesizer to generate the frequency needed to excite the Cs resonance. This difference frequency between the output of the 9.2 GHz synthesizer and the Cs resonance frequency is added to a second DDS and sent to the FLFC laboratory to be counted. With the comb stabilized to the Hg^+ light and the carrier-envelope offset frequency stabilized, the repetition rate of the comb can be related to the Hg^+ frequency

Hg^+ frequency. This repetition rate is measured with respect to a 1 GHz synthesizer that is referenced to a hydrogen maser via a stable quartz oscillator.

The frequency of the Cs standard is simultaneously measured with respect to the same hydrogen maser. In this way, the Cs standard provides a calibration of the hydrogen maser so that the Hg^+ frequency can be directly related to the SI realization of the second. The frequency of the Cs standard is measured with respect to the output of a stable 9.2 GHz synthesizer that is referenced to the frequency of the same hydrogen maser and quartz oscillator that are used in the measurement of the Hg^+ frequency. The output of the 9.2 GHz synthesizer is added to that of a direct digital frequency synthesizer (DDS) to generate the frequency that matches the Cs resonance. The deviations from the nominal value are added to a carrier near 10 MHz with a second DDS and sent to the FLFC laboratory, where they are measured with a frequency counter, simultaneous with the measurement of the Hg^+ frequency.

The ratio of the frequency of the Hg^+ standard with respect to Cs is determined by taking the ratio of the two frequencies measured with respect to the hydrogen maser. In this way, any drift in the frequency of the hydrogen maser is eliminated.

The Hg^+ frequency standard and NIST-F1 Cs standard have been described in detail in [7, 15, 17, 18] and [13, 14, 16], respectively. Here we limit our discussion of the two standards, providing only a summary of their associated corrections and uncertainties and a brief mention of those features specific to this experiment.

2.1 Cs frequency standard

The Cs frequency measured by the fountain relative to the hydrogen maser must be corrected in order to arrive at the unbiased Cs frequency. The largest bias of the NIST-F1 fountain is from the second-order Zeeman shift caused by the small magnetic field applied to the atoms in the fountain. To correct for this effect, the fractional frequency is shifted by $-36.2(1) \times 10^{-15}$.

The second largest correction comes from black-body radiation. The NIST-F1 apparatus is at room temperature and ambient black-body radiation leads to ac-Stark shifts of the Cs hyperfine transition frequency. These effects have been modeled and are corrected with a fractional shift in the frequency of $21.2(3) \times 10^{-15}$.

Finally, the frequency of the Cs standard is shifted due to the spin-exchange collisions of the Cs atoms. The Cs standard is operated at varying densities in order to balance the statistics with the systematic effects arising from spin-exchange collisions [16]. For this work the Cs standard was operated at a density approximately seven times higher than that used for the majority of the data collected during its accuracy evaluations. At this density the frequency standard has a fractional frequency instability of $2 \times 10^{-13} \tau^{-1/2}$, where τ is the averaging time in seconds and the correction from spin-exchange collisions is $2.00(33) \times 10^{-15}$ [13, 14].

The total fractional correction applied to the frequency of the Cs standard relative to the hydrogen maser was -13.0×10^{-15} . The total fractional frequency uncertainty in the Cs frequency standard during the time of these measurements is estimated to be 0.41×10^{-15} [13, 14].

2.2 Hg^+ frequency standard

The $^{199}\text{Hg}^+$ frequency standard is based on the $5d^{10}6s^2 S_{1/2} \rightarrow 5d^96s^2 D_{5/2}$ transition at 1.065×10^{15} Hz [7, 17, 18]. The radiation for the clock transition is produced by frequency quadrupling light produced from a fiber laser at 266 THz. The doubled light at 532 THz is prestabilized to a low-drift, high-finesse optical cavity and then steered to resonance with the Hg^+ .

Some of the stabilized light at 532 THz (563 nm) is sent through approximately 300 m of single-mode optical fiber to the femtosecond frequency comb. The frequency noise introduced by the fiber is suppressed by standard fiber-noise canceling techniques [15].

The systematic fractional frequency uncertainties are estimated to be less than 0.07×10^{-15} . The only corrected bias introduced in the Hg^+ frequency is due to the second-order Zeeman effect and leads to a fractional frequency shift of 1.1×10^{-15} .

2.3 Gravitational shift

The Hg^+ clock was located 4.51(10) m below the Cs standard and the FLFC. This difference in altitude gives a relative gravitational shift in the absolute frequency of the Hg^+ standard relative to the Cs standard. Based on the measured height difference, we apply a fractional correction of $+0.492(11) \times 10^{-15}$ to the measured frequency of the Hg^+ standard.

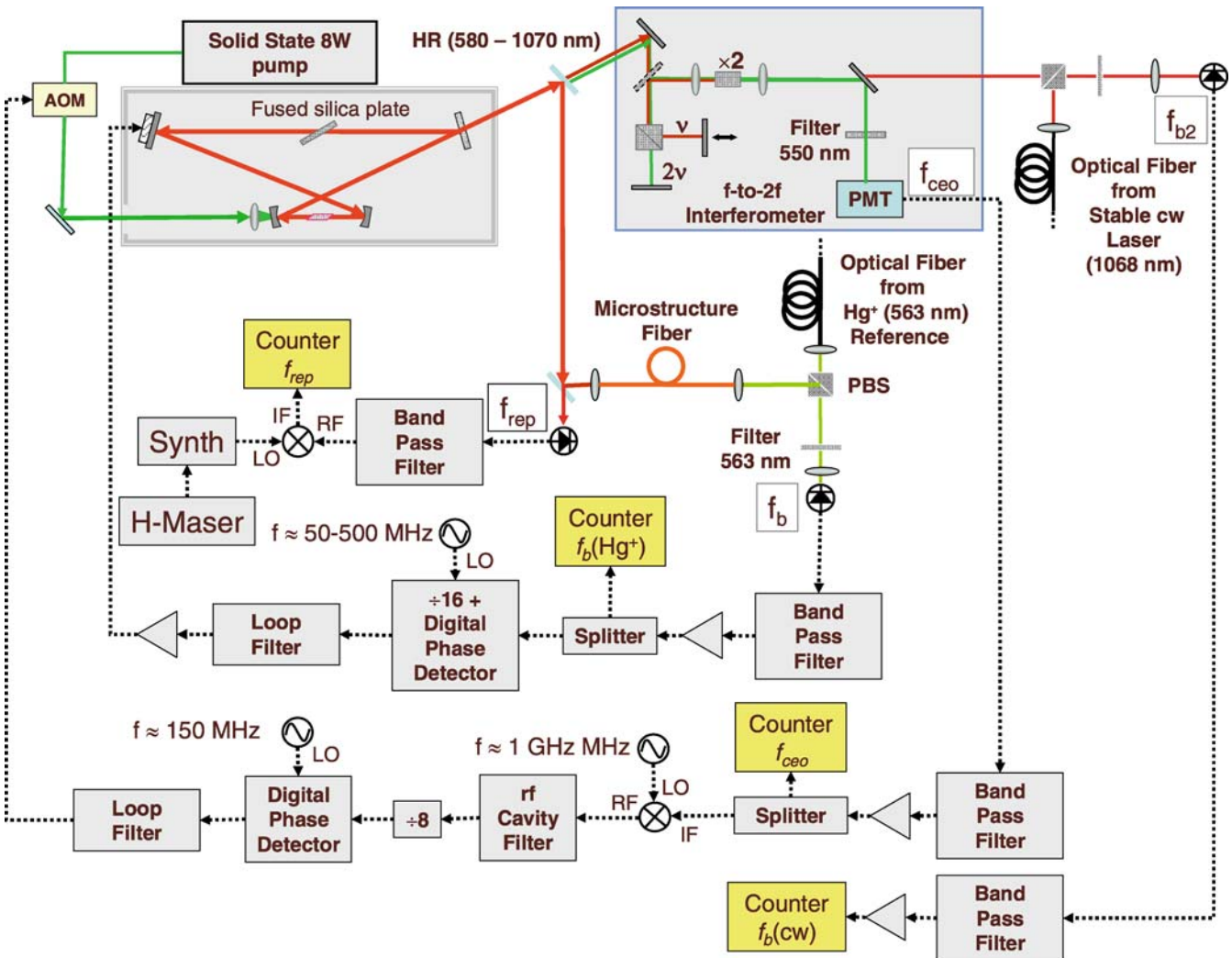


FIGURE 2 Block diagram showing the stabilization scheme of the FLFC for the $\text{Hg}^+ - \text{Cs}$ comparison

2.4 Optical-to-microwave conversion

The stabilization scheme of the FLFC is shown in Fig. 2. The comb used in the most recent measurements of the Hg^+ frequency is described in detail in [19]. The frequency comb is generated by a mode-locked laser based on Ti:sapphire with a repetition rate of about 1 GHz. The output of the laser spans an optical octave, allowing for the stabilization of the carrier-envelope offset frequency with a f -to- $2f$ self-referencing technique [1]. Part of the optical spectrum at approximately 1100 nm was frequency doubled and compared to the light directly produced by the laser near 550 nm. The doubled light and the direct light were interfered on a photomultiplier tube, resulting in a heterodyne beat signal, the frequency of which equals the carrier-envelope offset frequency, f_{ceo} . The carrier-envelope offset frequency can be coarsely adjusted by tilting a 1 mm piece of fused silica inside the laser cavity to change the cavity dispersion, and is servo controlled by changing the power of the laser pumping the FLFC by use of an acousto-optic modulator (AOM).

The comb was operated with the carrier-envelope offset frequency, f_{ceo} , phase locked at approximately 50 MHz. The signal-to-noise ratio of the beat signal was about 30 dB in

a 300 kHz resolution bandwidth. The detected beat note was mixed with the output of a frequency synthesizer operating near 1.2 GHz, and filtered through an rf cavity band-pass filter. The frequency of this signal was then divided by eight and it was sent to a digital phase detector, with the output of a second synthesizer operating at around 150 MHz, serving as the local oscillator. The error signal from the digital phase detector was conditioned with a loop filter and then sent to drive the amplitude of an rf signal controlling the pump power via an AOM. The carrier-envelope offset frequency was directly counted by a frequency counter to monitor for possible phase slips in the lock [20].

In order to achieve sufficient optical power and a clean spatial mode of the comb light for comparison with the Hg⁺ stabilized light at 563 nm, part of the comb output spectrum was broadened in a nonlinear microstructure fiber [21]. The output of the microstructure fiber was combined with the 563 nm light and interfered on a high-speed (≈ 300 MHz) photodiode. The 563 nm light used for the Hg⁺ frequency standard interferes with the different frequency components of the comb to produce a series of beat frequencies. The lowest heterodyne beat frequency was phase locked to a fixed frequency set by a synthesizer. The beat frequency was typically

between 35 and 200 MHz, and the signal-to-noise ratio was ≈ 30 dB in a 300 kHz resolution bandwidth. The beat note was filtered, amplified, and sent to a digital phase detector that included a 16-times divider. The error signal from the digital phase detector was sent to a loop filter and amplifier to control the cavity length via a piezoelectric transducer attached to one of the laser's cavity mirrors. The frequency of the beat note between the Hg^+ light and the nearest comb mode was also counted with a frequency counter to monitor phase slips in the lock.

With the carrier-envelope offset frequency and the frequency of the comb mode nearest the Hg^+ light phase locked, the repetition rate is given by

$$f_{\text{rep}} = \frac{f_{Hg^+} \pm f_b \pm f_{\text{ceo}}}{n}, \quad (1)$$

where f_{Hg^+} is the frequency of the Hg^+ light and f_b is the beat note between the Hg^+ light and the nearest frequency component of the comb with mode number n . The mode number, n , and the two signs are determined from the existing knowledge of the Hg^+ frequency.

An additional monitor of the stability of the Hg^+ light was provided by simultaneous measurement of the frequency of a second stable cw laser. Light from a fiber laser operating at 1068 nm, which is used for the aluminum ion frequency standard [22], was also interfered with light from the FLFC. The cw laser light was stabilized by frequency doubling a part of the light and locking it to a stable optical cavity at 534 nm. The light at 1068 nm had a fractional stability of $\approx 3 \times 10^{-15}$ in 1 s and a drift rate of less than 1 Hz/s [23]. A few milliwatts of this light was passed through approximately 300 m of optical fiber to the FLFC laboratory. Any noise introduced by this fiber link was actively canceled [15]. The heterodyne beat note of the nearest FLFC mode with this stable cw light was filtered, amplified, and counted simultaneously with the other signals. As will be discussed in Sect. 3, the higher fractional stability of this light compared to the hydrogen maser was more sensitive to phase slips in the locks and provided an important monitor for anomalous frequency excursions.

2.4.1 Optical uncertainties. The stability and accuracy of an optical synthesis process achieved with similar optical frequency combs has been tested to the 10^{-19} level by comparing two independent frequency combs phase locked to a common cw source [24]. There have been additional tests of the accuracy of the optical synthesis process that included sum and difference frequency generation using nonlinear crystals [25].

We tested the optical synthesis of the frequency comb used in this experiment by comparing the frequency of light from second-harmonic generation in a nonlinear crystal with the fundamental light [26]. Light at 1064 nm from a cw Nd:YAG laser was frequency doubled with a periodically poled lithium niobate crystal. An optical mode of the comb was phase locked to the frequency-doubled light at 532 nm in a manner identical to that used to stabilize the comb to the Hg^+ light. With the comb stabilized, the frequency of the 1064 nm light was measured by heterodyne detection with the nearest optical mode of the comb.

The harmonic relation of the two optical frequencies results in rejection of the common-mode noise. The remaining fractional instability places an upper limit on instabilities in the optical synthesis process due to frequency noise in the optical interference process, microstructure fiber, and phase locks of the laser. In addition, the accuracy of the optical synthesis process is tested by reproducing the exact ratio of the optical frequencies. We observed a fractional instability in the fundamental light relative to the doubled light of 2×10^{-17} in one second that averaged down slightly faster than $\tau^{-1/2}$ (Fig. 3). The ratio of the two frequency components yielded the expected value of two within a counter-limited uncertainty of 6×10^{-19} .

2.4.2 Photodetection uncertainties. While the optical instability of the comb is far below the statistical uncertainties of both of the frequency standards, the photodetection of the repetition rate introduces additional phase noise. This additional noise is a result of many different processes inherent in the conversion of the short optical pulse (~ 100 fs) to a much longer electronic pulse (~ 1 ns), such as the conversion of amplitude noise to phase noise, saturation effects within the photodiode, and laser-beam pointing noise [27]. The instability introduced due to this detection has been measured with similar detectors and combs and is estimated to be approximately 3×10^{-17} at around 10^5 s [28] (Fig. 3).

2.4.3 Electronic uncertainties. An upper limit on the stability of the 1 GHz synthesizer that was used to compare the FLFC repetition rate to the maser frequency (Fig. 1) was determined by mixing the output of the synthesizer with that of a second synthesizer referenced to the same maser. The relative fractional frequency instability of the two synthesizers was 3×10^{-14} in ten seconds and averaged down as $\tau^{-1/2}$ (Fig. 3). The two synthesizers had a relative inaccuracy of less than 3×10^{-16} .

In order to limit temperature drifts affecting the output frequency of the synthesizer, the synthesizer was enclosed in an insulated box through which cold water was circulated. The temperature inside the box was monitored throughout the experiment. The temperature dependence of the synthesizer was determined by introducing a rapid change in the temperature of the synthesizer and monitoring the frequency of the synthesizer relative to a second synthesizer. The synthesizer was measured to have a fractional frequency change of $6.0(1.4) \times 10^{-15} (\text{K/h})^{-1}$. This temperature coefficient was used along with the recorded temperature of the synthesizer to correct the measured repetition rate for drifts in the synthesizer frequency. The correction resulted in a fractional shift of the Hg^+ frequency of $0.08(2) \times 10^{-15}$.

The distribution amplifier and the cable used to send the maser signal to the FLFC laboratory were tested by sending the maser signal to the FLFC laboratory and then back to the fountain laboratory in an identical cable and comparing the frequency with the initial maser frequency directly in the fountain laboratory. The fractional stability of the maser distribution electronics measured in this way was 4×10^{-15} in ten seconds and showed a pronounced bump near 700 s (Fig. 3). The time scale of the increase in the noise is commensurate with the cycle of the air conditioning in the building.

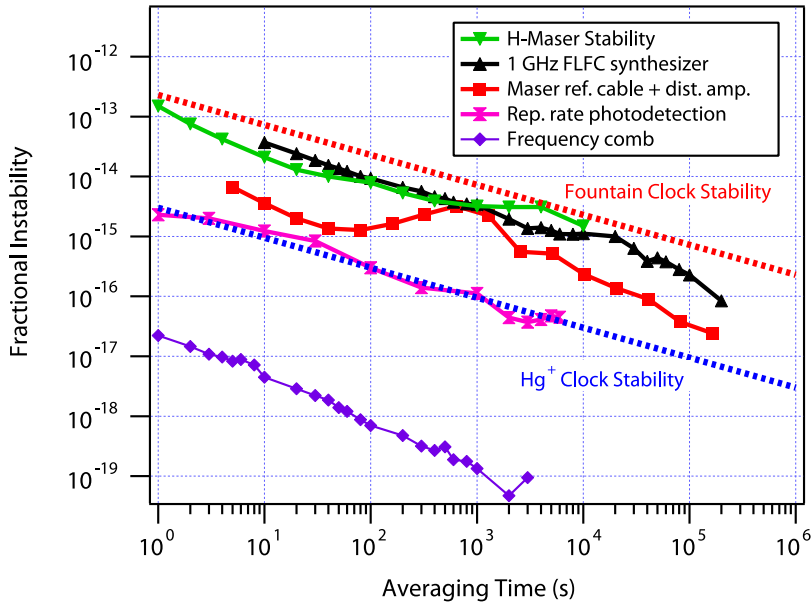


FIGURE 3 Frequency instabilities of the main components of the Hg^+ comparison

3 Analysis and results

The data for the March 2006 comparison were collected for $\approx 1.1 \times 10^5$ s over a 42 h period, corresponding to a duty cycle of $\approx 72\%$. This duty cycle was limited primarily by various technical aspects of the Hg^+ clock. The majority of the data were taken with a gate time for the frequency counters of 9.427 s. This value was chosen so that noise synchronous with 0.1 Hz and 60 Hz would average out. Additionally, some data were taken at 1 s and 29.427 s gate times.

3.1 Data processing

Throughout the course of the measurement, there were occasional anomalous frequency excursions due to a variety of different sources. The primary cause of these excursions was a frequency deviation in the Hg^+ light that occurred periodically with a time interval of ≈ 40 min. During these excursions the FLFC generally remained phase locked to the Hg^+ laser. These frequency deviations were related to a flaw in the Hg^+ clock laser system and were not due to any instability in the Hg^+ clock. In addition, there were occasional phase slips of the various locks throughout the experiment. Given these anomalous frequency excursions, the data processing is necessarily focused on determining which of the frequency excursions are intrinsic to either of the two frequency standards or measurement processes and which are a result of imperfections in the experiment.

The frequency excursions present in the Hg^+ light led to excursions in the frequency of the repetition rate measured relative to the hydrogen maser. These excursions were also present in the measurement of the frequency of the stable cw laser at 1068 nm. The relative fractional frequency instability between the Hg^+ stabilized comb and the stable cw laser was $\approx 2 \times 10^{-15}$ in ten seconds, while the relative fractional frequency instability of the Hg^+ stabilized comb and the hydrogen maser was $\approx 5 \times 10^{-14}$ in ten seconds. Consequently, the frequency of the stable cw laser provides a significantly more sensitive monitor for anomalous frequency excursions.

Figure 4 shows one hour of unprocessed data for the repetition rate and the stable cw laser, along with the data points that were considered anomalous excursions based on deviations in the repetition rate and the stable cw laser frequency.

Data that had an anomalous frequency excursion in any of the recorded frequencies were discarded. The criteria for the maximum allowable deviation were varied to determine the sensitivity of the final result on the data analysis. For the final analysis, data deviating by more than six times the standard deviation were discarded. In addition to excluding data that exhibited large frequency excursions, the data immediately preceding and following the anomalous point were discarded in order to ensure that the frequency excursion was completely removed. Varying the cutoff criteria between 6–15 sigma and keeping or discarding adjacent points changed the amount of data discarded over 11%–38%. However, the final results were statistically consistent. Overall, the variation of the final result with the separate analyses employing different filtering criteria was $\approx 0.04 \times 10^{-15}$. We adopt this as an estimate of the uncertainty introduced in the analysis process.

The phase-locked f_{ceo} and f_b frequencies are additive in the determination of the Hg^+ frequency resulting in fractional deviations which are equal to the measured excursion divided by the frequency of the Hg^+ light measured, 532 THz. The fractional deviations in f_{rep} and the Cs corrections to the maser frequency (steers) are normalized by 1 GHz and 9.2 GHz, respectively. The filtered time record of the fractional deviations in the counted signals is shown in Fig. 5.

3.2 Statistical uncertainties

The statistical uncertainties for the different frequency comparisons are shown in Fig. 6. The estimated statistical uncertainty of the Hg^+ standard is far below that of the Cs standard (Fig. 3) and we would expect the uncertainties of the Cs standard to dominate. However, the uncertainty in the Hg^+ /Cs comparison is larger than that of the Cs standard alone. The measurement of the maser frequency relative

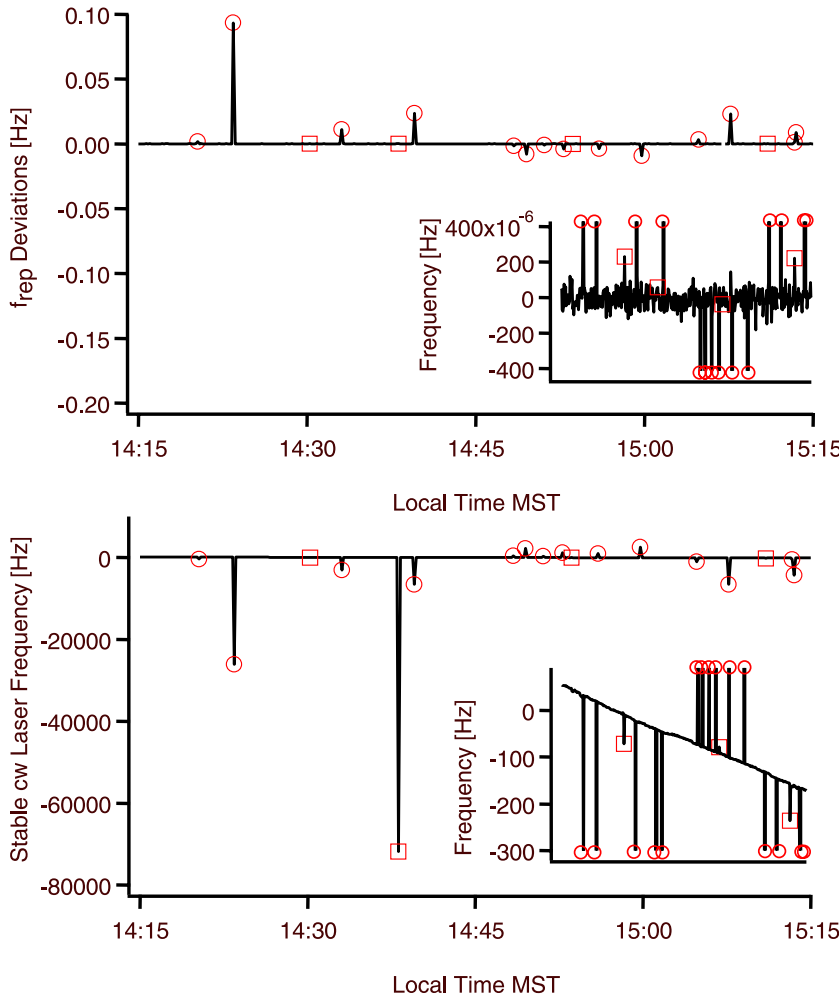


FIGURE 4 Relative frequencies of f_{rep} and the stable cw laser at 1068 nm for a representative hour of the data. *Upper plot* shows the relative frequency of f_{rep} offset from its mean value of ≈ 1 GHz. *Lower plot* shows the relative frequency of the stable cw laser offset from 281 THz. The circles indicate data that were considered outliers based on excursions in the repetition rate. Squares indicate data that were considered outliers based only on deviations in the stable cw laser. Insets show the same data with decreased frequency ranges

to the Cs standard performed in the FLFC lab was $\approx 20\%$ higher than the measurement of the maser frequency relative to the Cs standard done in the fountain lab. We believe that this additional noise can be attributed to the dead time between the counter measurements [29]. Indeed, data taken at different gate times in the FLFC lab had uncertainties equal to the uncertainty measured in the fountain lab. Unfortunately, the majority of the data were taken with a gate time that exhibited additional noise.

The fit of the fractional instability of the Hg⁺ frequency relative to that of Cs to a function of the form $A\tau^p$ yields a fractional instability of $3.0 \times 10^{-13} \tau^{-0.50}$, where τ is the averaging time in seconds. Evaluating this for the total averaging time of the experiment gives a fractional statistical uncertainty of 0.9×10^{-15} . This error is identical to that determined from the standard deviation divided by the square root of the number of points.

A summary of the uncertainties is shown in Table 1. The final fractional uncertainty is 1×10^{-15} , dominated by the statistical errors.

3.3 H-maser comparison

The hydrogen maser used in the experiment is part of a collection of five masers that are periodically calibrated with respect to the Cs NIST-F1 standard [30]. The five masers

Source	Uncertainty [10^{-15}]
Cs standard	0.41
Hg ⁺ standard	0.07
Gravitational shift	0.01
Optical uncertainties	< 0.01
Photodetection uncertainties	0.03
Synthesizer uncertainties	0.3
Analysis uncertainties	0.04
Statistical uncertainty	0.9
Final uncertainty	1

TABLE 1 Uncertainties in the March 2006 Hg⁺ frequency comparison with Cs NIST-F1 frequency standard

are compared continuously to each other in order to determine the drifts of the masers and to calibrate their frequencies. The Hg⁺ frequency can therefore be determined directly from the frequency of the maser by use of the daily-averaged maser-maser calibration. The calculation of the Hg⁺ frequency in this way provides a redundancy check. The frequency obtained by this method agrees with that obtained via the more direct comparison with the Cs standard to within 0.5×10^{-15} .

3.4 Final result and comparison with previous measurements

The final value for the most recent (9 March 2006) absolute frequency measurement of the Hg⁺ frequency stan-

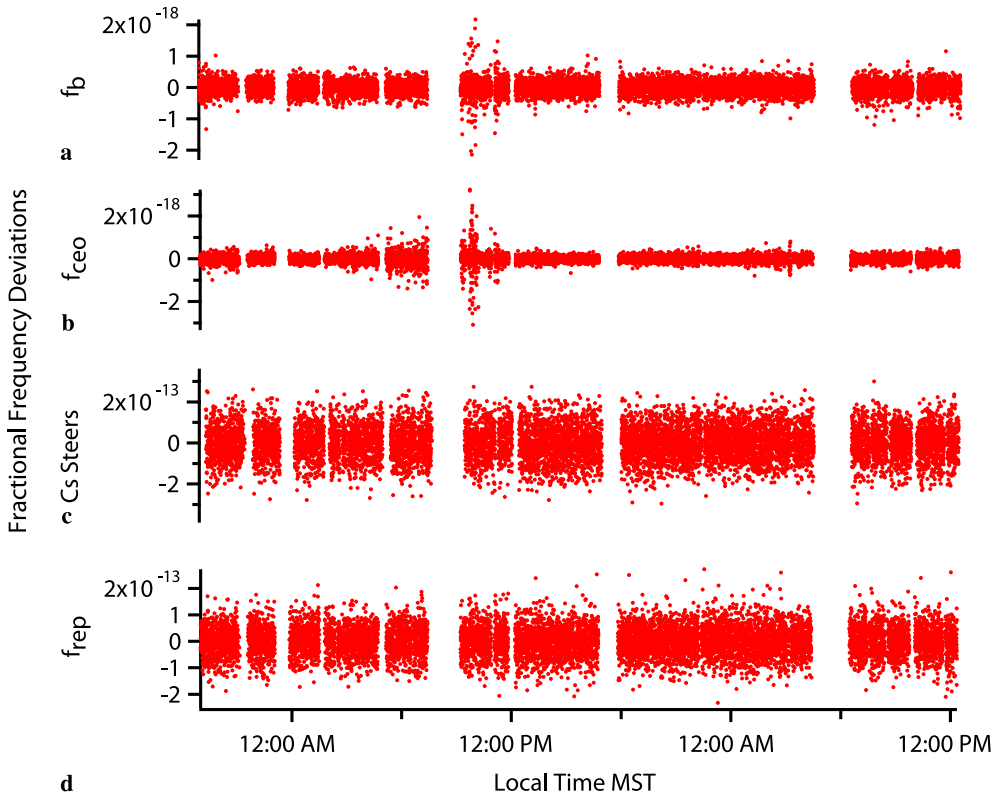


FIGURE 5 Time record of the counted fractional frequency deviations for (a) phase-locked optical beat between Hg^+ light and FLFC, (b) phase-locked carrier-envelope offset frequency, (c) Cs frequency relative to hydrogen maser, (d) repetition rate of FLFC. The gate time of the counters for this data was 9.472 s and there are 10289 points

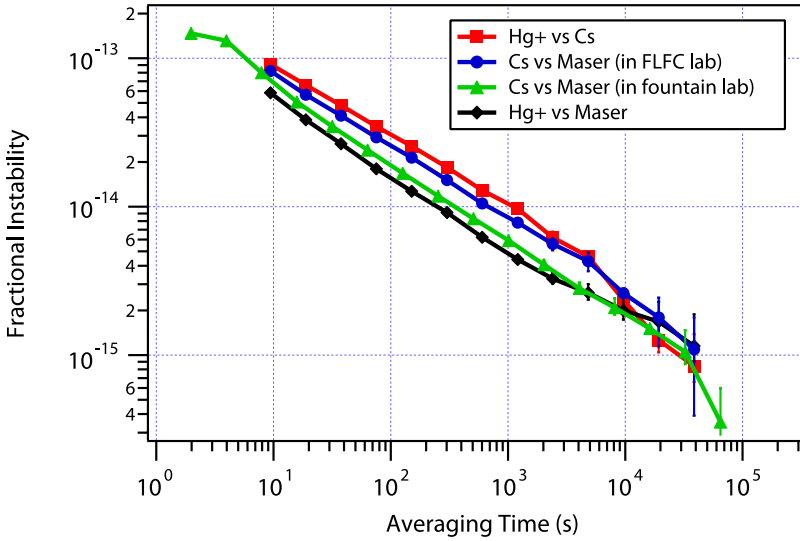


FIGURE 6 Allan deviations for the frequency comparisons

dard is

$$f(\text{Hg}^+) = 1\,064\,721\,609\,899\,145.89(1.06) \text{ Hz}. \quad (2)$$

This result is in good agreement with the previously published values [7, 17]. Table 2 and Fig. 7 show all of the absolute frequency measurements of the Hg^+ transition. These measurements have been used to obtain stringent limits on possible variations in fundamental constants as well as tests of local position invariance [6], in addition to development of frequency standards.

The compilation of the data to arrive at a final mean is complicated by the evolution of the experimental techniques and the presence of systematic uncertainties that are due to

random fluctuations (type A) and those that are constant for a group of measurements (type B). Furthermore, the type B uncertainties in the Hg^+ clock have changed significantly over the time of the measurements.

Table 2 shows the statistical uncertainties, and the type A and type B uncertainties, for both the Hg^+ frequency standard and the rf standard (hydrogen maser or Cs fountain clock).

For the purposes of combining the errors, the data were broken up into data taken prior to 2005 and those taken after 2004. For all of the data, the dominant type A systematic uncertainty for the Hg^+ clock was due to fluctuations in the magnetic field leading to fluctuations in the second-order Zeeman shift of the transition [17]. The data taken prior

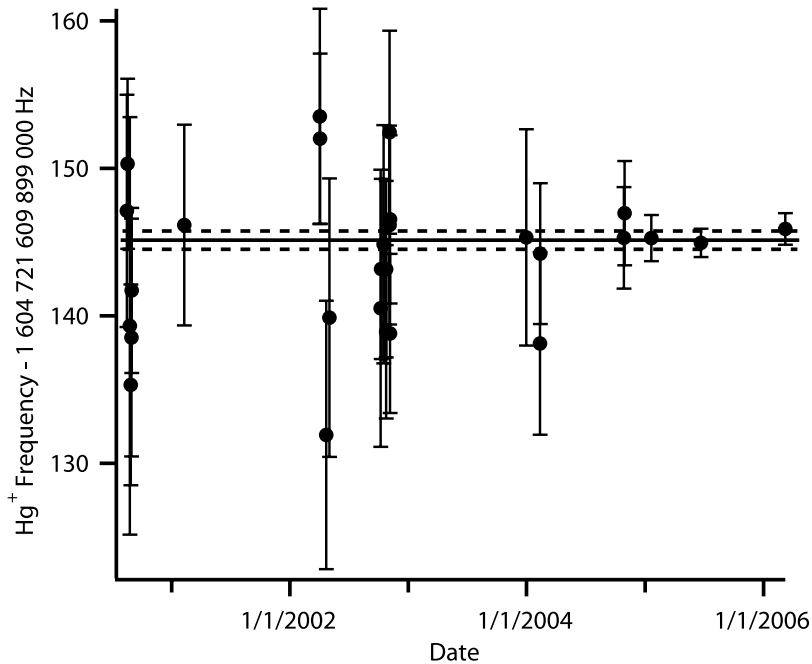


FIGURE 7 Historical record of absolute frequency measurements of the Hg^+ transition. The *solid line* shows the mean and the *dashed line* indicates the error on the mean

Date	Statistical		Hg^+		Cs/maser	Conversion	Hg^+	Total
		Type A	Type B	Type A	Type B		frequency	uncertainty
8/16/00	7.5	2.2	2.8	2.1	< 1	< 1	147.12	8.59
8/18/00	5.3	2.2	2.8	2.1	< 1	< 1	150.32	6.71
8/25/00	13.8	2.2	2.8	2.1	< 1	< 1	139.32	14.41
8/28/00	6.4	2.2	2.8	2.1	< 1	< 1	135.32	7.61
8/30/00	7.7	2.2	2.8	2.1	< 1	< 1	138.52	8.76
8/31/00	5.1	2.2	2.8	2.1	< 1	< 1	141.72	6.56
2/9/01	5.2	2.2	2.8	4.3	< 1	< 1	146.15	7.62
4/3/02	5.8	2.2	2.8	4.3	< 1	< 1	153.53	8.06
4/4/02	3.7	2.2	2.8	4.3	< 1	< 1	152.02	6.70
4/23/02	8.0	2.2	2.8	4.3	< 1	< 1	131.92	9.72
5/3/02	8.4	2.2	2.8	4.3	< 1	< 1	139.88	10.05
10/8/02	8.3	2.2	2.8	4.3	< 1	< 1	140.52	10.0
10/9/02	4.2	2.2	2.8	4.3	< 1	< 1	143.18	7.00
10/17/02	6.8	2.2	2.8	4.3	< 1	< 1	144.86	8.77
10/25/02	4.1	2.2	2.8	4.3	< 1	< 1	143.16	6.90
10/25/02	3.9	2.2	2.8	4.3	< 1	< 1	138.92	6.80
11/4/02	5.1	2.2	2.8	4.3	< 1	< 1	146.16	7.56
11/4/02	5.3	2.2	2.8	4.3	< 1	< 1	152.46	7.68
11/6/02	3.1	2.2	2.8	4.3	< 1	< 1	138.80	6.39
11/6/02	3.6	2.2	2.8	4.3	< 1	< 1	146.54	6.66
12/31/03	7.0	0.10	2.8	2.1	< 1	< 1	145.32	7.79
2/11/04	5.2	0.10	2.8	3.2	< 1	< 1	138.12	6.72
2/12/04	3.4	0.10	2.8	3.2	< 1	< 1	144.22	5.45
10/27/04	2.6	0.05	2.8	2.0	< 1	< 1	145.29	4.32
10/29/04	2.8	0.05	2.8	1.9	< 1	< 1	146.96	4.40
1/20/05	0.84	0.05	1.2	0.45	0.35	0.25	145.28	1.59
6/22/05	0.82	0.05	0.07	0.29	0.35	0.25	144.94	0.96
3/09/06	0.95	0	0.07	0.33	0.35	0.30	145.89	1.06

TABLE 2 Absolute frequency measurements and uncertainties of the Hg^+ transition. Listed are the uncertainties from the different aspects of the measurements in Hz (see text for details) along with the final frequency and uncertainty. The data is grouped by measurement. The last three points were taken over more than one day and an average date is given. The Hg^+ frequency is reported as $f(\text{Hg}^+) - 1 604 721 609 899 000 \text{ Hz}$

to 2005 were originally reported with a type B uncertainty of 10 Hz, dominated by the electric quadrupole shift of the $\text{Hg}^+ {}^2D_{5/2}$ ($F = 0, M_F = 0$) state [17]. This uncertainty has been revised and reduced to 1 Hz, based on a recent measurement of the quadrupole moment [31] and the recorded measurements of the secular frequencies of the trap. With this reduction, type B uncertainties for the Hg^+ frequency are dominated by the uncertainty in the second-order Zeeman

coefficient at a level of 2.6 Hz [17], giving a total type B uncertainty of 2.8 Hz of the Hg^+ standard for these data. The rf source for the data taken before 2005 was a hydrogen maser the frequency of which was corrected by use of the daily-averaged maser–maser calibration, as discussed in Sect. 3.3. The uncertainty in the correction is a type A uncertainty as tabulated in Table 2. These data were combined by taking a mean weighted by the statistical and type A uncertainties

and adding the 2.8 Hz type B uncertainty in quadrature with the error on the mean.

The data taken after 2004 were acquired as direct, real-time comparisons versus the Cs frequency standard, as outlined above. Consequently, there is a significant reduction in uncertainties associated with the rf source. As discussed in Sect. 2.1, the dominant type A systematic uncertainty is due to the shifts from spin-exchange collisions, and the dominant type B uncertainties are from the black-body radiation and second-order Zeeman shift [14]. The uncertainties in the Hg⁺ clock also dramatically decreased for these measurements. With the exception of the data taken in January 2005, the uncertainties in the Hg⁺ clock were pushed down to an insignificant level.

With the improvements in the two frequency standards for the last two points, the uncertainties from the optical-to-microwave conversion process are no longer negligible and are included in the analysis. As discussed in Sect. 2.4, these uncertainties are dominated by the type A uncertainties in the synthesizers used in the conversion. These data were combined by taking a mean weighted by the statistical uncertainties, the type A uncertainties for the Cs and Hg⁺ standards, the type B uncertainty for the Hg⁺ standard, and the uncertainties due to the optical-to-microwave conversion. The type B uncertainty for the Hg⁺ standard was included in the weight because of its dramatic reduction between the January data and the final two data sets. The improvements in the Hg⁺ frequency standard resulted in the type B uncertainty for the January data being uncorrelated with the type B uncertainty for the last two data sets. After this weighted mean, the type B uncertainties from the Cs standard were added in quadrature.

The weighted mean of the frequencies as determined from the data sets described above gives a final value for the Hg⁺ transition of

$$f(\text{Hg}^+) = 1\,064\,721\,609\,899\,145.30(69) \text{ Hz}. \quad (3)$$

4 Perspective and outlook

The accuracy attained for the frequency of the Hg⁺ transition will greatly aid in the development of future optical frequency standards. The improved level of stability of the Hg⁺ frequency standard relative to rf standards provides a superior secondary standard that will quickly allow for the evaluation of future optical frequency measurements. In addition, this improved stability will allow for optical-to-optical frequency comparisons with relative fractional precision approaching 10^{-17} in the near future.

The uncertainty in the optical-to-microwave conversion process used in the measurement of the Hg⁺ optical frequency standard with respect to the Cs frequency standard remains below the statistical uncertainties of the measurement and the systematic uncertainties from the Cs standard. The dominant uncertainties in the optical-to-microwave conversion process are related to the photodetection of the repetition rate and the quality of the synthesizer against which the repetition rate is compared. These uncertainties are not present in the comparison of two optical standards. Indeed, the uncertainty due to the optical synthesis process in the comparison of

two optical standards will not rely on detecting the repetition rate, and the uncertainties related to the photodetection process and synthesizer will be eliminated. For such a comparison we estimate the uncertainty from the optical-to-optical conversion process to be less than 10^{-19} , well below the anticipated inaccuracies of the next generation of optical frequency standards.

ACKNOWLEDGEMENTS The authors thank E. Donley, T. Rosenband, D. Hume, D. Wineland, and J. Torgerson for their contributions to this work and E. Donley and C. Oates for their careful reading of the paper. This work is a contribution of NIST and is not subject to U.S. Copyright. Funding for this work was provided by NIST, NASA, and LANL.

REFERENCES

- 1 D.J. Jones, S.A. Diddams, J.K. Ranka, A. Stentz, R.S. Windeler, J.L. Hall, S.T. Cundiff, *Science* **288**, 635 (2000)
- 2 R. Holzwarth, T. Udem, T.W. Hänsch, J.C. Knight, W.J. Wadsworth, P.S.J. Russell, *Phys. Rev. Lett.* **85**, 2264 (2000)
- 3 T. Udem, R. Holzwarth, T.W. Hänsch, *Nature* **416**, 233 (2002)
- 4 L. Hollberg, S. Diddams, A. Bartels, T. Fortier, K. Kim, *Metrologia* **42**, S105 (2005)
- 5 M.M. Boyd, A.D. Ludlow, S. Blatt, S.M. Foreman, T. Ido, T. Zelevinsky, J. Ye, *Phys. Rev. Lett.* **98**, 083002/1 (2007)
- 6 T.M. Fortier, N. Ashby, J.C. Bergquist, M.J. Delaney, S.A. Diddams, T.P. Heavner, L. Hollberg, W.M. Itano, S.R. Jefferts, K. Kim, F. Levi, L. Lorini, W.H. Oskay, T.E. Parker, J. Shirley, J.E. Stalnaker, *Phys. Rev. Lett.* **98**, 070801/1 (2007)
- 7 W.H. Oskay, S.A. Diddams, E.A. Donley, T.M. Fortier, T.P. Heavner, L. Hollberg, W.M. Itano, S.R. Jefferts, M.J. Delaney, K. Kim, F. Levi, T.E. Parker, J.C. Bergquist, *Phys. Rev. Lett.* **97**, 020801/1 (2006)
- 8 M. Takamoto, F.-L. Hong, R. Higashi, Y. Fujii, M. Imae, H. Katori, *J. Phys. Soc. Japan* **75**, 104302/1 (2006)
- 9 R. Le Targat, X. Baillard, M. Fouché, A. Brusch, O. Tcherbakoff, G.D. Rovera, P. Lemonde, *Phys. Rev. Lett.* **97**, 130801/1 (2006)
- 10 E. Peik, B. Lipphardt, H. Schnatz, T. Schneider, C. Tamm, S.G. Karshenboim, *Phys. Rev. Lett.* **93**, 170801/1 (2004)
- 11 H.S. Margolis, G.P. Barwood, G. Huang, H.A. Klein, S.N. Lea, K. Szymancie, P. Gill, *Science* **306**, 1355 (2004)
- 12 M. Fischer, N. Kolachevsky, M. Zimmermann, R. Holzwarth, Th. Udem, T.W. Hänsch, M. Abgrall, J. Grüner, I. Maksimovic, S. Bize, H. Marion, F. Pereira Dos Santos, P. Lemonde, G. Santarelli, P. Laurent, A. Clairon, C. Salomon, M. Haas, U.D. Jenischura, C.H. Keitel, *Phys. Rev. Lett.* **92**, 230802/1 (2004)
- 13 T.P. Heavner, S.R. Jefferts, E.A. Donley, J.H. Shirley, T.E. Parker, *IEEE Trans. Instrum. Meas.* **54**, 842 (2005)
- 14 T.P. Heavner, S.R. Jefferts, E.A. Donley, J.H. Shirley, T.E. Parker, *Metrologia* **42**, 411 (2005)
- 15 B.C. Young, R.J. Rafac, J.A. Beall, F.C. Cruz, W.M. Itano, D.J. Wine land, J.C. Bergquist, in *Proceedings of the XIV International Conference on Laser Spectroscopy*, Innsbruck, Austria, ed. by R. Blatt (World Scientific, Singapore, 1999), pp. 61–70
- 16 S.R. Jefferts, J. Shirley, T.E. Parker, T.P. Heavner, D.M. Meekhof, C. Nelson, F. Levi, G. Costanzo, A. De Marchi, R. Drullinger, L. Hollberg, W.D. Lee, F.L. Walls, *Metrologia* **39**, 321 (2002)
- 17 S. Bize, S.A. Diddams, U. Tanaka, C.E. Tanner, W.H. Oskay, R.E. Drullinger, T.E. Parker, T.P. Heavner, S.R. Jefferts, L. Hollberg, W.M. Itano, J.C. Bergquist, *Phys. Rev. Lett.* **90**, 150802/1 (2003)
- 18 S.A. Diddams, Th. Udem, J.C. Bergquist, E.A. Curtis, R.E. Drullinger, L. Hollberg, W.M. Itano, W.D. Lee, C.W. Oates, K.R. Vogel, D.J. Wineland, *Science* **293**, 825 (2001)
- 19 T.M. Fortier, A. Bartels, S.A. Diddams, *Opt. Lett.* **31**, 1011 (2006)
- 20 T. Udem, J. Reichert, T.W. Hänsch, M. Kourogi, *Opt. Lett.* **23**, 1387 (1998)
- 21 J.K. Ranka, R.S. Windeler, A.J. Stentz, *Opt. Lett.* **25**, 25 (2000)
- 22 P.O. Schmidt, T. Rosenband, C. Langer, W.M. Itano, J.C. Bergquist, D.J. Wineland, *Science* **309**, 749 (2005)
- 23 B.C. Young, F.C. Cruz, W.M. Itano, J.C. Bergquist, *Phys. Rev. Lett.* **82**, 3799 (1999)
- 24 L.-S. Ma, Z. Bi, A. Bartels, L. Robertsson, M. Zucco, R.S. Windeler, G. Wilpers, *Science* **303**, 1843 (2004)

- 25 M. Zimmermann, C. Gohle, R. Holzwarth, T. Udem, T.W. Hänsch, Opt. Lett. **9**, 310 (2004)
- 26 J. Stenger, H. Schnatz, C. Tamm, H.R. Telle, Phys. Rev. Lett. **88**, 073601/1 (2002)
- 27 E.N. Ivanov, S.A. Diddams, L. Hollberg, IEEE J. Sel. Top. Quantum Electron. **9**, 1059 (2003)
- 28 L.-S. Ma, Z. Bi, A. Bartels, K. Kim, L. Robertsson, M. Zucco, R.S. Windeler, G. Wilpers, C. Oates, L. Hollberg, S.A. Diddams, IEEE J. Quantum Electron. **QE-43**, 139 (2007)
- 29 P. Lesage, IEEE Trans. Instrum. Meas. **IM-32**, 204 (1983)
- 30 T.E. Parker, S.R. Jefferts, T.P. Heavner, E.A. Donley, Metrologia **42**, 423 (2005)
- 31 W.H. Oskay, W.M. Itano, J.C. Bergquist, Phys. Rev. Lett. **94**, 163001/1 (2005)